

1 Synthesis, Characterization, and Catalytic Properties of Cationic Hydrogels Containing Copper(II) and Cobalt(II) Ions

3 Lucía Victoria Lombardo Lupano,[†] Juan Manuel Lázaro Martínez,^{*,‡} Lidia Leonor Piehl,[§]
4 Emilio Rubín de Celis,[§] Rosa María Torres Sánchez,^{||} and Viviana Campo Dall'Orto^{*,†}

5 [†]IQUIFIB-CONICET & Departamento de Química Analítica y Físicoquímica, Facultad de Farmacia y Bioquímica, Universidad de
6 Buenos Aires, Junín, 956 (1113) CABA, Argentina

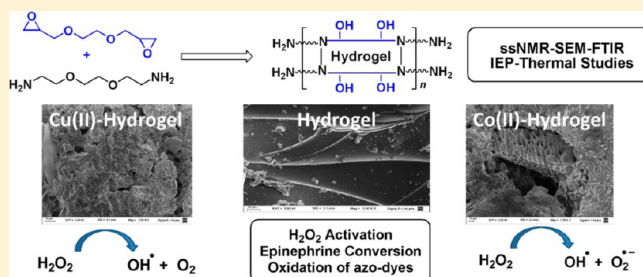
7 [‡]CONICET, Av. Rivadavia 1917 (1033), CABA, Argentina & Departamento de Química Orgánica, Facultad de Farmacia y
8 Bioquímica, Universidad de Buenos Aires, Junín, 956 (1113) CABA, Argentina

9 [§]Departamento de Fisicomatemática, Facultad de Farmacia y Bioquímica, Universidad de Buenos Aires, Junín, 956 (1113) CABA,
10 Argentina

11 ^{||}CETMIC-CONICET, Camino Centenario y 506, M. B. Gonnet, 1897, Argentina

12 **S** Supporting Information

13 **ABSTRACT:** Here, we report the synthesis and character-
14 ization of a hydrogel based on ethylene glycol diglycidyl ether
15 (EGDE) and 1,8-diamino-3,6-dioxaoctane (DA). Chemically
16 stable Co(II) and Cu(II) coordination complexes were
17 prepared with this nonsoluble polyelectrolyte, *poly*(EGDE-
18 DA), and studied by *ss*-NMR, FT-IR, thermogravimetry, and
19 microscopy. Mesopores were found in all the samples, the
20 thermal stability of the polymer matrix was highly affected by
21 the presence of metal ions, and the ¹³C CP-MAS spectrum for
22 the Cu(II)-complex evidenced a significant increase in the
23 reticulation degree by Cu(II) ions. The catalytic activity of
24 these materials on H₂O₂ activation was studied by electron spin resonance (ESR). The Co(II)-*poly*(EGDE-DA)/H₂O₂
25 heterogeneous system produced O₂, an anion superoxide (O₂^{•-}), and a hydroxyl radical (OH[•]), which diffused into the solution
26 at the time that a decrease in pH was detected. In the same way, the Cu(II)-*poly*(EGDE-DA)/H₂O₂ heterogeneous system
27 produced O₂ and OH[•]. H₂O₂ activation by the *poly*(EGDE-DA) complexes with Co(II) and Cu(II) were applied on the
28 decolorization of solutions of the azo-dye methyl orange (MO). In the presence of 63 mM H₂O₂, 87% of MO was removed in 10
29 min with Cu(II)-*poly*(EGDE-DA) and in 110 min with Co(II)-*poly*(EGDE-DA). In addition, the pharmaceutical product
30 epinephrine was partially oxidized to adrenochrome by the O₂^{•-} released from the Co(II)-*poly*(EGDE-DA)/H₂O₂ heterogeneous
31 system.



1. INTRODUCTION

32 The coordination of a polymeric ligand by a transition metal
33 ion is an efficient way to obtain processable materials with
34 unique and valuable properties. Polymer networks offer new
35 possibilities to scientists for the creation of artificial materials.
36 In recent years, hydrogels with chelating ligands attracted the
37 attention for industrial applications.¹ In particular, polyelec-
38 trolyte and polyampholyte hydrogels have become of great
39 interest in the macromolecular chemistry area due to their
40 versatility as excellent adsorbents of chemical compounds.²
41 Stimuli-sensitive hydrogels are used in a variety of novel
42 applications, including controlled drug delivery, immobilized
43 enzyme systems, separation processes, fuel cells, and sensor
44 development.^{3,4}

45 We have previously demonstrated that nonsoluble polymers
46 can be prepared from ethylene glycol diglycidyl ether (EGDE)
47 using methacrylic acid (MAA) and/or *N*-heterocycles. The
48 synthetic process involves the opening of the epoxy groups

49 from EGDE by the reaction with MAA, and a peroxide-initiated
50 radical polymerization of MAA segments covalently bound to
51 EGDE to give a polyelectrolyte [*poly*(EGDE-MAA)]. When
52 imidazole (IM) is added to the reaction mixture, the epoxy
53 groups are opened up by both the carboxylic acid of the MAA
54 and the pyridine-type nitrogen of the *N*-heterocycle, yielding a
55 polyampholyte [*poly*(EGDE-MAA-IM)].⁵⁻⁷ When EGDE and
56 IM are mixed in the absence of the radical polymerization
57 initiator [*poly*(EGDE-IM)], a polyelectrolyte is also synthe-
58 sized. The respective polyampholytes and polyelectrolytes were
59 derived from a variety of *N*-heterocycles such as 2-
60 methylimidazole (2MI), pyrazole (PYR), and triazole (TRZ).^{8,9}

61 These materials offer the versatility to complex different
62 metal ions due to the presence of the imidazole ligand,

Received: December 17, 2013

Revised: January 28, 2014

63 carboxylic, and hydroxyl groups in the structure. In Cu(II)-
64 poly(EGDE-MAA-IM) and Cu(II)-poly(EGDE-MAA-2MI)
65 complexes, the imidazole ring has been found to be the main
66 group involved in metal ion uptake and the carboxylic group
67 appears to have a coordinating role only at high concentrations
68 of the metal ion.^{10,11} A similar behavior has been reported for
69 the complexation of copolymers from unsaturated carboxylic
70 acids and vinylimidazole with Cu(II)¹⁰ and for Cu(II)
71 coordination to some peptides.¹¹

72 Functional materials are often made by the synergistic
73 combination of organic and inorganic components. Cu(II) and
74 Co(II) complexes with these hydrophilic, nonsoluble matrices
75 have been demonstrated to activate hydrogen peroxide (H₂O₂)
76 to produce free radicals and dioxygen.^{12,13} When Cu(II) and
77 Co(II) complexes are used as heterogeneous catalysts, the
78 formation of hydroxyl radical (OH•) and anion superoxide
79 (O₂^{•-}), respectively, is evidenced by electron spin resonance
80 (ESR). Both reactive species have been proven to oxidize the
81 azo-dye methyl orange (MO), and O₂^{•-} effectively converts
82 epinephrine into a partially oxidized product named adreno-
83 chrome.^{12,13}

84 Herein, we report a synthetic strategy to prepare
85 polyelectrolytes based on a diepoxy monomer and a bifunc-
86 tional primary amine, using EGDE and DA as reactants.
87 Because it is well-established that the coordination compounds
88 of nonsoluble polymers with Co(II) and Cu(II) play a key role
89 in H₂O₂ activation, we explored performance of the new
90 complexes as heterogeneous catalysts. Although H₂O₂ is an
91 attractive reagent of low environmental impact because water is
92 the only byproduct, it is a rather slow oxidizing agent in the
93 absence of activators.¹⁴ Nowadays, the advanced oxidation
94 processes by means of hydroxyl radicals are widely recognized
95 as highly efficient treatments for recalcitrant wastewater.¹⁵ At
96 the same time, H₂O₂ is being applied in eco-friendly
97 technologies dealing with the synthesis of value-added chemical
98 products, which involve oxidations under mild conditions.¹⁶ To
99 explore the environmental and industrial applications of the
100 novel complexes on H₂O₂ activation, we used two different
101 organic substrates: MO (a synthetic dye found in wastewater)
102 and epinephrine (a model compound of pharmaceutical
103 precursors).

2. EXPERIMENTAL SECTION

104 **2.1. Materials and Reagents.** Ethylene glycol diglycidyl ether
105 (EGDE; 50 wt % in ethylene glycol dimethyl ether) was from TCI
106 America. 1,8-Diamino-3,6-dioxaoctane (DA), epinephrine bitartrate,
107 and 5,5-dimethyl-1-pyrroline-N oxide (DMPO) were purchased from
108 Sigma–Aldrich. Superoxide dismutase (SOD) was from Biosidus
109 (Buenos Aires, Argentina). Acetonitrile from Baxter was of HPLC
110 grade.

111 CoSO₄ and cobalt acetate were purchased from Mallinckrodt.
112 CuSO₄·2H₂O, Na₂SO₄, and H₂O₂ (30 wt %) were acquired from
113 Merck (Darmstadt, Germany). Methyl Orange (MO) was from Santa
114 Cruz Biotechnology, Inc. Soybean peroxidase (SBP) was extracted
115 from soybean seed coat with water.

116 Water was distilled with a FIGMAY glass apparatus (Córdoba,
117 Argentina). All other reagents were of analytical grade.

118 **2.2. Instruments.** High-resolution ¹³C solid-state spectra for the
119 polymers were recorded using the ramp {¹H}→{¹³C} CP-MAS (cross-
120 polarization and magic angle spinning) sequence with proton
121 decoupling during acquisition. All the *solid-state* nuclear magnetic
122 resonance (*ss*-NMR) experiments were performed at room temper-
123 ature in a Bruker Avance II-300 spectrometer equipped with a 4 mm
124 MAS probe. The operating frequencies for protons and carbons were
125 300.13 and 75.46 MHz, respectively.^{12,17}

The FT-IR spectra of the polymers and their copper complexes 126
were recorded on a Nicolet 380 spectrometer using KBr pellets. SEM 127
imaging and EDS were carried out with a scanning electron 128
microscope field emission SEM (Zeiss Gemini DSM 982) operated 129
at a 0.3 kV acceleration voltage and an INCA Energy (Oxford 130
Instrument), respectively. Elemental analysis was performed with a 131
Carlo Erba EA 1108 device. A nitrogen adsorption isotherm was 132
collected at 77 K on a Micromeritics Gemini 2360 system. Specific 133
surface area was calculated using the BET (Brunauer–Emmett– 134
Teller) equation. The electron spin resonance (ESR) spectra were 135
obtained at 20 °C using an X-band ESR Spectrometer Bruker EMX 136
plus (Bruker Instruments, Inc., Berlin, Germany). Partial pressure of 137
O₂ was measured with an Orbisphere A1100-Oxygen Sensor. UV– 138
visible spectrophotometric measurements were made on a Hewlett- 139
Packard instrument, HP 8452A model with diode array. 140

The isoelectric point (IEP) value was obtained by diffusion 141
potential determination as described elsewhere.¹⁸ Electromotive 142
force (EMF) measurements were carried out with a Keithley 616 143
digital electrometer instrument with Metrohm calomel electrodes. 144
Potentiometric titration of the polyelectrolyte was performed with a 145
HANNA Instrument pH meter as elsewhere.^{5,6} 146

2.3. Synthesis of Poly(EGDE–DA). An aliquot of 176 μL (1.2 147
mmol) of 1,8-diamino-3,6-dioxaoctane (DA) and 0.4 mL (1.28 mmol) 148
of ethylene glycol diglycidyl ether (EGDE; 50 wt % in ethylene glycol 149
dimethyl ether) was mixed with 0.4 mL of acetonitrile. The solution 150
was placed in a tube glass and thermostatted at 60 °C for 24 h. The 151
product was placed at 20 °C, milled, washed three times with distilled 152
water, and dried at 60 °C during 24 h. The polyelectrolyte was used 153
without further purification. 154

2.4. Swelling Equilibrium. Equilibrium swelling measurements 155
were performed in triplicate at pH 3.00 with an ionic strength (*I*) of 156
0.50 and <0.001 and at pH 9.80 with *I* = 0.50. 157

An amount of the polyelectrolyte was immersed in a measured 158
volume of the corresponding aqueous solution and kept for 2 days to 159
reach equilibrium. Swollen material was separated by filtration, 160
weighed, and dried at 90 °C until constant weight. The dried material 161
was cooled at 20 °C in a desiccator and weighed again. The swelling 162
degree and water content were calculated as elsewhere.^{5,6} 163

**2.5. Differential Scanning Calorimetry (DSC) and Thermog- 164
ravimetry (TG).** The glass transition temperature (*T_g*) values of the 165
polyelectrolyte and its copper and cobalt complexes were measured on 166
a Shimadzu 60 type differential scanning calorimeter (DSC) at a rate 167
of 15 °C min⁻¹ during the second heating trace in the calorimeter 168
under a nitrogen purge. 169

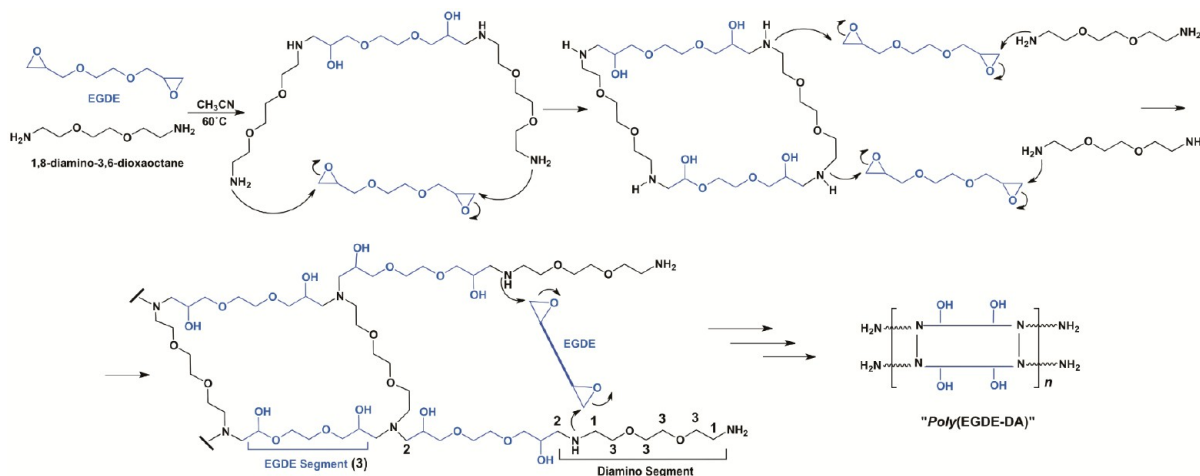
Thermogravimetric measurements were carried out with a TA 170
Instrument SDT Q600, under nitrogen flux over a temperature range 171
from 30 to 400 °C, with a heating rate of 10 °C min⁻¹. The average 172
sample size was 10 mg. 173

2.6. Cobalt Uptake. Cobalt binding studies were performed with 174
0.0500 g of polyelectrolyte and 4.0 mL of CoSO₄ solution in a 5.0–40 175
mM concentration range. The samples were centrifuged and filtered 176
after 48 h of contact time at 24 °C. Free Co(II) concentration at the 177
equilibrium in each supernatant solution could be determined 178
spectrophotometrically since Co²⁺ forms a coordination compound 179
with SCN⁻ in the presence of HCl and acetone, which absorbs 180
radiation at 622 nm.¹⁹ 181

2.7. Copper Uptake. Copper binding studies were performed with 182
0.0250 g of polyelectrolyte and 4.0 mL of CuSO₄ solution in a 4.0–70 183
mM concentration range. The samples were centrifuged and filtered 184
after 48 h of contact time at 24 °C. Free Cu(II) concentration in each 185
supernatant solution could be determined spectrophotometrically 186
since Cu(NH₃)₄²⁺ (formed by ammonium hydroxide addition) 187
absorbs radiation at 640 nm. The isotherm and kinetic parameter 188
sets were determined by nonlinear regression. The algorithm based on 189
the Gauss–Newton method was used. The error function employed to 190
evaluate the fit was the second order corrected Akaike criterion 191
(AIC_c).^{20,21} 192

**2.8. Preparation of Co(II)-poly(EGDE-DA) and Cu(II)-poly(- 193
EGDE-DA).** The complexes were prepared mixing 0.5000 g of polymer 194
powder and 40 mL of 70 mM CoSO₄ solution for Co(II)-poly(EGDE- 195

Scheme 1. Synthesis of Poly(EGDE-DA) and the Representative Structure of the Product



196 DA) and of 140 mM CuSO₄ solution for Cu(II)-poly(EGDE-DA), in
197 distilled water at 24 °C for 48 h.

198 The samples were then centrifuged, washed with three 20 mL
199 portions of distilled water to remove the cation weakly adsorbed on
200 the particles, filtered, dried at 60 °C, and milled in a mortar. The last
201 portion of water from the wash step did not present detectable
202 amounts of free cation in solution, when each one was tested by the
203 colorimetric methods described in Cobalt Uptake and Copper Uptake.
204 The loading capacity for each cation under the mentioned conditions
205 was 15.2 mg Co(II) g⁻¹ and 170 mg Cu(II) g⁻¹ (0.258 mmol Co(II)
206 g⁻¹ and 2.67 mmol Cu(II) g⁻¹, respectively).

207 **2.9. Measurement of H₂O₂ Concentration.** This peroxide reacts
208 with phenol and 4-aminoantipyrine in the presence of soybean
209 peroxidase (SBP), giving a product that absorbs radiation at 505
210 nm.^{12,22} An amount of 0.0500 g of each complex was suspended in 50
211 mL of 42 mM H₂O₂. The concentration of H₂O₂ was monitored as a
212 function of time from 20 μL samples of the reaction.^{12,22}

213 **2.10. Measurement of Free Radicals by ESR.** The initial H₂O₂
214 concentration was set close to 60 mM. Higher concentration levels of
215 H₂O₂ were expected to be less efficient in oxidative processes due to
216 possible deleterious effects on the polymeric catalysts.^{12,13} An amount
217 of 0.0500 g of each complex was suspended in 50 mL of 63 mM H₂O₂
218 solution and the production of free radicals was followed by ESR. The
219 experiment was also performed in the presence of SOD with an
220 activity of 200 units mL⁻¹ added to the system before H₂O₂.

221 Aliquots of 32 μL taken at different times of reaction were mixed
222 with 16 μL of 3 M DMPO (spin trap), and the continuous wave (CW)
223 ESR spectra of the DMPO spin adducts were recorded at 20 °C, 3 min
224 after the end of incubation, in an X-band ESR Spectrometer Bruker
225 EMX Plus (Bruker Biospin GmbH, Germany). The spectrometer
226 settings and simulations conditions were reported previously by
227 Lombardo Lupano et al.¹²

228 In parallel, the measurements of O₂ partial pressure were made in
229 triplicate with a O₂ sensor, at 10 min of reaction.

230 **2.11. Methyl Orange Decolorization.** An amount of 0.1000 g of
231 Co(II)-poly(EGDE-DA) or Cu(II)-poly(EGDE-DA) was suspended in
232 100 mL of 42 μM MO and 63 mM H₂O₂ solution. The medium of
233 reaction was distilled water. The absorbance of the solution was
234 monitored as a function of time at 464 nm. For turbidity correction,
235 the absorbance was measured at 700 nm and subtracted to the
236 absorbance at 464 nm. The control of MO adsorption on the catalyst
237 was made in the absence of H₂O₂.

238 For the evaluation of the chemical stability of the catalysts on
239 reutilization, the experiment with MO was repeated three times with
240 the same recycled catalyst and new aliquots of solution.

241 The experiments conducted to study the MO degradation by
242 soluble free radicals were made with 0.1000 g of Co(II)-poly(EGDE-
243 DA) or Cu(II)-poly(EGDE-DA) suspended in 80 mL of 79 mM H₂O₂
244 solution. Here, the H₂O₂ solution was activated during 10 min with

the solid particles of each complex. Then, the suspension was filtered, 245
the supernatant was recovered and mixed with 20 mL of 210 μM MO 246
solution, and the MO concentration in the resulting solution was 247
monitored as a function of time. 248

For the detection of cobalt or copper intermediate species 249
catalytically active, 0.1000 g of Co(II)-poly(EGDE-DA) or Cu(II)- 250
poly(EGDE-DA) were put in contact with 100 mL of 63 mM H₂O₂ 251
solution for 10 min. The suspension was centrifuged, the supernatant 252
was discarded, the particles were washed with three portions of 253
distilled water, and they were not dried. The activated particles of the 254
catalyst were put in contact with 100 mL of 42 μM MO solution, and 255
the MO concentration was monitored as a function of time by visible 256
spectrophotometry. 257

Additional controls and tests were made by changing the chemical 258
composition of the medium of reaction or the mass of catalyst (g) to 259
volume of solution (L) ratio. A 0.1 M Na₂SO₄ solution was used as an 260
alternative medium. 261

For the experiments with equimolar amounts of catalytic sites 262
(0.644 mmol of sites L⁻¹), 0.2500 g of Co(II)-poly(EGDE-DA) were 263
suspended in 100 mL of 42 μM MO, and 0.0241 g of Cu(II)- 264
poly(EGDE-DA) were suspended in 100 mL of 42 μM MO. H₂O₂ was 265
added to initiate the catalytic reaction, and it was absent in the 266
adsorption control. 267

2.12. Epinephrine Oxidation. An amount of 0.0400 g of Co(II)- 268
poly(EGDE-DA) was suspended in 20 mL of 2 mM epinephrine and 269
46 mM H₂O₂ solution (higher concentrations of H₂O₂ were proved to 270
be less effective). The absorbance of the solution was monitored as a 271
function of time at 480 nm. For turbidity correction, the absorbance 272
was measured at 700 nm and subtracted to the absorbance at 480 nm. 273

A control experiment of epinephrine oxidation in the homogeneous 274
system was made with a solution of 2 mM epinephrine and 46 mM 275
H₂O₂. Another control experiment was made with 0.0400 g of Co(II)- 276
poly(EGDE-DA) suspended in 20 mL of 2 mM epinephrine in absence 277
of H₂O₂. This experiment was repeated with previous and continuous 278
bubbling of argon in the solution to displace the dissolved O₂. 279

3. RESULTS AND DISCUSSION

3.1. Synthesis and Characterization of the Polyelectrolyte. The novel hydrogel poly(EGDE-DA) was synthesized 281
in a one-step batch synthetic strategy using ethylene glycol 282
diglycidyl ether (EGDE) and 1,8-diamino-3,6-dioxaoctane 283
(DA). Initially, the nitrogen atom of DA caused the opening 284
of the epoxy group present in the EGDE molecule with the 285
concomitant proton transfer and the generation of a hydroxyl 286
group and a secondary amine (Scheme 1). Then, the pendant 287 s1
amino groups may react with other oxirane rings to give rise to 288
a hydrogel system with hydroxyl groups together with different 289

290 primary, secondary, and tertiary amines, which may adopt a
 291 positive charge in acidic medium. The presence of linear
 292 polyamines is only possible as short pendant chains at the end
 293 of the cross-linked network. In this sense, the nonsoluble
 294 behavior of the poly(EGDE-DA) in strong acidic medium
 295 indicated that the cross-linked structure is more significant than
 296 the linear polyamine segment.

297 This makes this system an interesting polyelectrolyte material
 298 and also an attractive coordination hydrogel against metal ions
 299 through the nitrogen and/or oxygen ligands. Scheme 1 exhibits
 300 the most representative chemical structure of this product.

301 The dried and milled polymer rendered 95%, with an
 302 elemental composition of N, 5.1%; C, 52.1%; H, 9.2%. From
 303 this result, it can be concluded that 1.82 mmol of DA residues
 304 were bound to the EGDE segment per gram of polymer. The
 305 number of titrable basic sites (represented as $-R_2N$, where R
 306 can be either H or organic chain) was 0.978 mmol g^{-1} ,
 307 determined by potentiometry. The titration curve and the
 308 acid–base properties of *poly*(EGDE-DA) are presented in
 309 Figure S1 and the Discussion of Figure S1 of the Supporting
 310 Information.

311 The diffusion potential determination gave an IEP of 10.5,
 312 indicating that the particles were positively charged up to that
 313 pH value (Figure S2 of the Supporting Information).

314 **3.2. Characterization by FT-IR and *ss*-NMR.** The
 315 polymer material was characterized using FT-IR and *ss*-NMR
 316 spectroscopy, and the results are shown in Figure S3 of the
 317 Supporting Information and in Figure 1, respectively. The FT-

2930 cm^{-1} (stretching of C–H), and $\sim 3400\text{ cm}^{-1}$ (stretching
 of the N–H/O–H groups).

The ^{13}C CP-MAS spectrum of the material gave only
 information related to the methylene groups bound directly to
 the oxygen atom at 70 ppm ($-CH_2-O-$). These carbons are
 both present in the “EGDE” and “diamino” segments (Figure
 1), but no information regarding the carbons bound to nitrogen
 was obtained.

3.3. Swelling Degree. The water content of polyelec-
 trolytes is related to charge solvation. The repulsive forces
 among fixed charges and the osmotic pressure due to
 counterions induce network expansion.^{23,24} The results for
 this new material are summarized in Table S1 of the Supporting
 Information. At pH 3.0, the basic groups of polymeric units are
 protonated (Figure S1 of the Supporting Information),
 acquiring a positive charge and forcing the segments to stretch
 out. This creates more room for solvent between the cross-links
 and allows the hydrogel to swell.

The results at pH 3.0 show the dependence of the swelling
 degree on I .²⁵ At low I , the counterions (responsible for the
 osmotic effect) are assumed to remain in the matrix, making the
 electrostatic repulsion between chains the dominant effect on
 expansion. At higher I , the Donnan effect caused a decrease in
 swelling because of the additional shielding of the fixed charges
 on the chain by the additional diffusible counterions. At pH 9.8,
 the swelling degree did not change significantly, finding about
 50% of the basic residues protonated due to the low apparent
 acid dissociation constant of the $-R_2NH^+$ (discussion of Figure
 S1 of the Supporting Information).

3.4. Adsorption of Cu(II) and Co(II). The mechanism of
 copper uptake was explored by analyzing the results of the
 adsorption isotherm for the polyampholyte at 20 °C. Four
 isotherm models (Temkin, Langmuir, Dubinin–Radushkevich
 (D–R), and Freundlich) were used to fit the experimental
 adsorption data by nonlinear regression (Table 1).

The best fit of experimental adsorption data was obtained
 with Temkin, Langmuir, and D–R isotherms (Figure S4 of the
 Supporting Information), according with the evidence ratio
 based on the Akaike criterion.²⁰ The Freundlich model had no
 statistical support due to its significantly larger residual sum of
 squares.

The negative change in free energy (ΔG°) derived from K_L^{-1}
 in the Langmuir model indicated the spontaneous nature of the
 adsorption (Table 1).

The Temkin model assumes that the heat of adsorption of all
 molecules in the layer will decrease linearly rather than
 logarithmically with coverage due to adsorbate/adsorbate
 interactions.²⁶

$$q_e = \frac{RT}{b_T} \ln(K_T C_e) \quad (1)$$

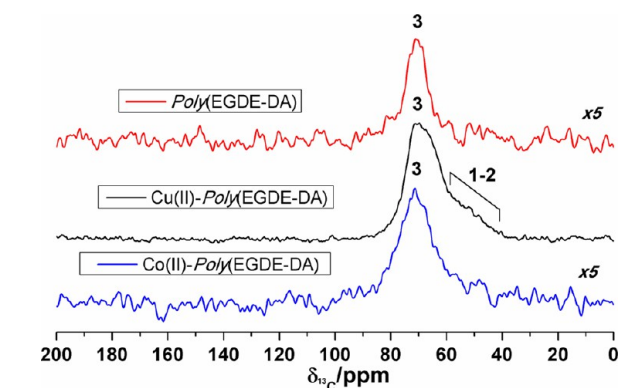


Figure 1. ^{13}C CP-MAS spectra for *poly*(EGDE-DA) and for its Cu(II)-
 and Co(II) complexes containing 125.0 and 12.5 mg of metal ion per
 gram of polymer, respectively. The assignments correspond to those in
 Scheme 1.

318 IR spectrum of *poly*(EGDE-DA) indicated a lack of good
 319 resolution with the presence of amorphous particles of the gel.
 320 However, some bands were observed at 1112 cm^{-1} (due to the
 321 stretching of the C–O ether groups), 1460 and 1650 cm^{-1}
 322 (deformation motion of $-O-CH_2-$ and $-N-H$, respectively),

Table 1. Isotherm Parameters for Cu(II) Adsorption on *Poly*(EGDE-DA). Regression coefficients, values of AICc Criterion and Evidence Ratio for Temkin, Langmuir, Dubinin–Radushkevich (D–R), and Freundlich Models^a

| model | parameters | | | R^2 | AIC _c | evidence ratio |
|------------|---------------------------------------|--|--|--------|------------------|----------------|
| Temkin | $K_T: 1.37 \pm 0.46\text{ L mg}^{-1}$ | $b: 0.1300 \pm 0.0069\text{ kJ mol}^{-1}$ | | 0.9676 | 61.35 | 1 |
| Langmuir | $q_m: 151.4 \pm 3.6\text{ mg g}^{-1}$ | $K_L: 41.1 \pm 5.5\text{ mg L}^{-1}$ | $\Delta G^\circ: -17.880 \pm 0.058\text{ kJ mol}^{-1}$ | 0.9574 | 62.78 | 2.03 |
| D–R | $q_m: 225 \pm 11\text{ mg g}^{-1}$ | $B_D: 1.80 \times 10^{-3} \pm 0.10 \times 10^{-3}\text{ mol}^2\text{ kJ}^{-2}$ | $E: 16.67 \pm 0.46\text{ kJ mol}^{-1}$ | 0.9500 | 66.96 | 16.42 |
| Freundlich | $K_F: 42.2 \pm 5.1$ | $n: 6.05 \pm 0.61$ | | 0.9175 | 73.74 | 489.50 |

^a q_e (mg g^{-1}) vs C_e (mg L^{-1}) except for in the D–R model, in which C_e is in $g\text{ g}^{-1}$.

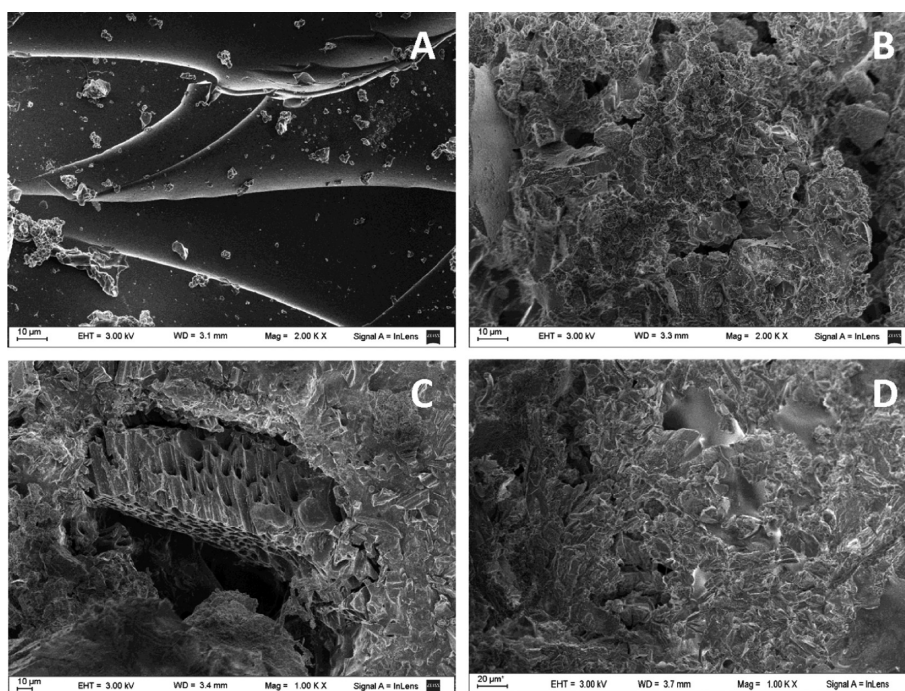


Figure 2. SEM images of (A) *poly*(EGDE-DA), (B and C) Co(II)-*poly*(EGDE-DA), and (D) Cu(II)-*poly*(EGDE-DA).

372 where q_e is the adsorption capacity in equilibrium with the
373 corresponding C_e , which is the concentration of metal ion.

374 The D–R isotherm is a semiempirical equation which was
375 originally developed for subcritical vapors in microporous
376 solids, where the adsorption process follows a pore-filling
377 mechanism:

$$378 \quad q_e = q_m e^{-B_D \varepsilon^2} \quad (2)$$

379 where q_m is the maximum amount of adsorbate that can be
380 adsorbed in micropores, B_D is a constant related to the energy,
381 and ε is the Polanyi potential.^{12,27}

382 The value estimated for q_m was 225 mg of Cu(II) per gram of
383 polymer (3.54 mmol g⁻¹), significantly higher than that
384 predicted by Langmuir model (151.4 mg g⁻¹) (Table 1).

385 Equation 2 is generally applied to express the adsorption
386 mechanism with a Gaussian energy distribution onto a
387 heterogeneous surface. The approach is usually applied to
388 distinguish the physical and chemical adsorption of metal ions
389 by means of eq 3

$$390 \quad E = \frac{1}{\sqrt{2B_D}} \quad (3)$$

391 where E is the mean free energy of sorption,²⁸ whose
392 magnitude is a way to estimate the type of sorption process.²⁹
393 The E value observed was higher than 16 kJ mol⁻¹ K⁻¹,
394 suggesting the coordination of Cu(II) with the primary,
395 secondary, and/or tertiary amine-type groups, –OH residues,
396 and/or O atoms of the polymer. The green color of the
397 particles of Cu(II)-*poly*(EGDE-DA) is another evidence of
398 coordination (Figure S5 of the Supporting Information). In
399 addition, the ESR spectra of Cu(II)-*poly*(EGDE-DA) also
400 suggested that different coordination modes could coexist in
401 this material, being the N atoms more significant than O atoms
402 in the uptake of Cu(II) (Figure S6 and Discussion of Figure S6
403 in the Supporting Information).⁹

The loading capacity for Co(II) was estimated in 15.2 ± 2.9 404
mg g⁻¹ (0.258 ± 0.049 mmol g⁻¹). When the Co(II) uptake 405
equilibrium was studied, the material was saturated in all the 406
range of concentrations tested, giving a brown product (Figure 407
S5 of the Supporting Information). 408

3.5. Characterization of the Complexes by FT-IR and 409
ss-NMR. The resulting Co(II)- and Cu(II)-complexes were 410
spectroscopically characterized through FT-IR and ss-NMR 411
experiments (Figure S3 of the Supporting Information and 412
Figure 1, respectively). First, the FT-IR spectra presented a 413
better resolution than with the initial material without metal 414
ions. In particular, the copper complex showed a better spectral 415
resolution, when one considers that this material is more rigid 416
than the original unloaded hydrogel and could be easily milled 417
in small particles, being more appropriate for spectroscopic 418
determinations. In addition, the effects of the cross-linking 419
induced by metal ions was more evident in the case of copper 420
because *poly*(EGDE-DA) presented a higher amount of Cu(II) 421
per gram of polymer than the Co(II) complex, which 422
reinforced the interactions between the polymer chains and 423
the metal ion. For the Cu(II)-complex, a new band was 424
observed at 603 cm⁻¹, associated with the stretching of the S– 425
O bond from SO₄²⁻ arising as a counterion of copper. The 426
wagging of the N–H bond at 880 cm⁻¹ and also the stretching 427
band of the N–H bond at 3566–3600 cm⁻¹ were well-resolved. 428
In the case of the Co(II) complex, the FT-IR spectrum showed 429
bands similar to those of the Cu(II)-complex, but the signals 430
were vanished because the low amount of cobalt ion uptake was 431
not the optimal to mill in small particles as in the case of 432
copper. 433

The ¹³C CP-MAS spectrum for the Cu(II)-complex shows 434
the missing methylene carbons in the *poly*(EGDE-DA) bound 435
to nitrogen as a shoulder of the principal signal at around 50 436
ppm (C_{1,2}, Figure 1), as a consequence of the cross-linking of 437
the system by the copper ions. In general, the signal-to-noise 438
ratio was improved. However, even when the copper ion 439
induced the reticulation of the system, the paramagnetic ion 440

also enhanced the relaxation behavior on the carbons in the proximity of the metal ion ($-\text{CH}_2-\text{NH}_2-\text{Cu}$). For that reason, the signal of the mentioned methylene at around 50 ppm was not completely resolved. Finally, in the case of the Co(II) complex, the ^{13}C CP-MAS spectrum was similar to that of the unloaded material, without a significant increase in the reticulation degree as in the *poly*(EGDE-DA).

3.6. DSC and TG Analyses. The thermal behavior of the complexes and the hydrogel was studied by DSC and TG analyses. The glass transition temperature (T_g) was determined by DSC curves during the second scan over the temperature range of 20–160 °C (Figure S7 of the Supporting Information). The T_g value obtained for the polyelectrolyte was 120.0 °C, while that for the Cu(II)-complex containing 131 mg of Cu(II) per gram of polymer was 169.5 °C. This shift to higher temperature values was due to the stabilization of the d -electron of the copper ion on coordination, as expected,^{30–34} and it was also another fact of the cross-link between the polymer chains and the copper ion. For the Co(II) complex, the T_g value was 134.1 °C, and it was lower than in the case of copper, in concordance with the low amount of cobalt ions adsorbed to the polymer material, reducing the cross-linking between the polymer chains and cobalt ions.

In addition, the thermogravimetric analysis (TG-DTG) showed an initial loss of weight due to the evaporation of water in all the cases, coincident with an endothermic peak in the first DSC scan. *Poly*(EGDE-DA) initiated its thermal decomposition at ~ 300 °C with a maximal loss of weight at 377 °C. The Cu(II)-complex presented a lower decomposition temperature than the unloaded polymer (~ 200 °C). The presence of the paramagnetic Cu(II) ion center caused changes in the electronic density in the proximity of the metal ion which weakened the chemical bonds and decreased the thermal stability of the polymer backbone at high temperatures, regardless of the concentration of Cu^{2+} adsorbed, as it is shown in the TG profile for the Cu(II) complexes containing 50 or 131 mg of the metal ion per gram of material (Figure S8 of the Supporting Information).^{30–34} Moreover, the Co(II) complex showed a TG profile similar to that of any of the copper complexes, indicating that the thermal stability of the polymer matrix is highly affected by the presence of a metal ion even at a low concentration. The fact that all the polymers doped with Cu(II) or Co(II) have lower decomposition temperature than the undoped materials indicated that the metal ion acted as a catalyst, accelerating and reducing the thermal degradation of the polymer matrix.

3.7. SEM and EDS Analysis. SEM images were obtained without surface modifications. The complexes with Cu(II) and Co(II) were characterized using SEM to evidence the surface morphological changes when compared with the polyelectrolyte. The SEM image of *poly*(EGDE-DA) depicted in Figure 2 is regular in contrast with the surfaces of the complexes, which exhibit a significant difference in homogeneity degree. On the other hand, the magnification of Co(II)-*poly*(EGDE-DA) shows a regular arrangement of 5 to 10 μm diameter macropores, not evident in the other samples (Figure 2C).

The identities of copper and cobalt were manifested in EDS spectra (Figure S9 of the Supporting Information). In agreement with the FT-IR results, the presence of sulfur in the samples was detected because CoSO_4 and CuSO_4 were used to obtain the respective complexes. The presence of SO_4^{2-} evidenced the existence of fixed positive charges on the surface

of the particles, coming from Co(II), Cu(II), and/or $-\text{R}_2\text{NH}^+$. This SO_4^{2-} could eventually be exchanged by other anions.

The BET surface area for each material is presented in Table S2 of the Supporting Information.

The specific surface area determined by N_2 adsorption was very low in all the cases due to the hydrophilic nature of the polymer. This accessible area increased with the number of cations adsorbed, probably as a consequence of the network expansion due to electrostatic repulsion. *Poly*(EGDE-DA) can be classified as a mesoporous material, with an adsorption average pore width at the lower limit for this category.³⁵ The significantly larger mesopores in its complex with Cu(II) would also arise from the expansion of the chains.

3.8. H_2O_2 Activation by the Metal Complexes. We have previously demonstrated that the complexes of EGDE-based polymers with Cu(II) and Co(II) have catalytic activity on H_2O_2 activation.^{12,13} In the present study, the Co(II)-*poly*(EGDE-DA) and Cu(II)-*poly*(EGDE-DA) were tested as catalysts for the activation of this peroxide. Both complexes were put in contact with 42 mM H_2O_2 , and the concentration of H_2O_2 was monitored as a function of time. In each case, the reaction followed pseudo-first order kinetics (Figure S10 of the Supporting Information).

$$[\text{H}_2\text{O}_2]_t = [\text{H}_2\text{O}_2]_{\text{deg}} \times e^{-kt} \quad (4)$$

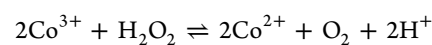
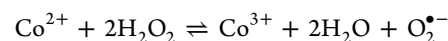
For Co(II)-*poly*(EGDE-DA), the estimated parameters and their standard deviations (S.D.) were 41.86 mM $[\text{H}_2\text{O}_2]_{\text{deg}}$ (S.D.: 0.31) and $3.7 \times 10^{-3} \text{ min}^{-1} k$ (S.D.: 0.2×10^{-3}), with $R^2 = 0.9735$. For Cu(II)-*poly*(EGDE-DA), the estimated parameters were 41.82 mM $[\text{H}_2\text{O}_2]_{\text{deg}}$ (S.D.: 0.19) and $9.0 \times 10^{-4} \text{ min}^{-1} k$ (S.D.: 0.6×10^{-4}), with $R^2 = 0.9597$. The H_2O_2 concentration decay was slow but evident. The evolution of gas bubbles from the surface of the particles of Co(II)-*poly*(EGDE-DA) with the addition of H_2O_2 and only in the presence of immobilized Co(II) was indicative of the formation of O_2 , which coincided with the decrease in pH of one unit at 10 min of reaction (Table S3 of the Supporting Information).

The Co(II)-*poly*(EGDE-DA)/ H_2O_2 heterogeneous system also produced free radicals that diffused to the solution and were detected by spin trapping experiments with DMPO (Figure 3A).

The simulation and fits of the experimental spectrum allowed establishing the presence of two species: DMPO/OOH and DMPO/OH adducts from anion superoxide ($\text{O}_2^{\bullet-}$) and hydroxyl radical (OH^\bullet), respectively (Figure S11A of the Supporting Information).³⁶

The addition of the enzyme superoxide dismutase (SOD) to the medium of reaction gave rise to a spectrum with the characteristic shape of DMPO/OH (Figure S12 of the Supporting Information).

On the basis of this experimental evidence, we propose a reaction of H_2O_2 activation catalyzed by immobilized Co(II), with the production of O_2 , $\text{O}_2^{\bullet-}$, and H^+ :³⁷



where OH^\bullet is an intermediate in $\text{O}_2^{\bullet-}$ formation.

The presence of OH^\bullet as a minor product of the reaction and as the main product after the addition of SOD, could be explained by splitting the first step as follows:

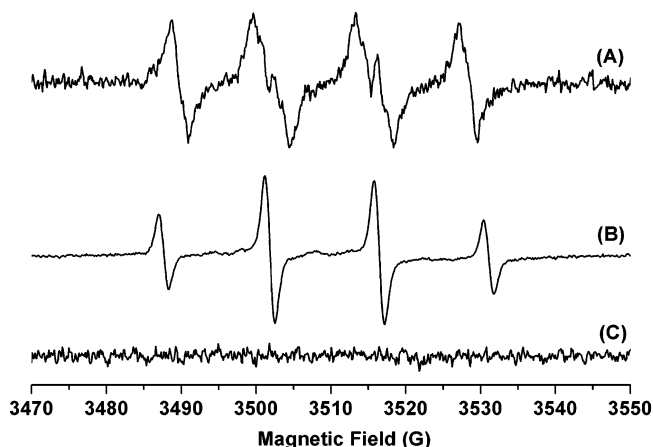
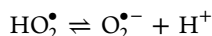
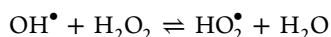
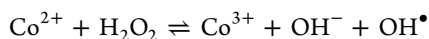


Figure 3. Experimental CW ESR in band X spectra from spin trapping experiments with DMPO 10 min after the addition of H_2O_2 . Heterogeneous systems: (A) $\text{Co(II)-poly(EGDE-DA)}/63 \text{ mM } \text{H}_2\text{O}_2$; (B) Heterogeneous system: $\text{Cu(II)-poly(EGDE-DA)}/63 \text{ mM } \text{H}_2\text{O}_2$. The ESR spectrum of DMPO is depicted as C.

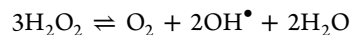


559 The stage of OH^\bullet degradation must be the slowest in the
560 presence of SOD, which would explain the observation of the
561 DMPO/OH signal.

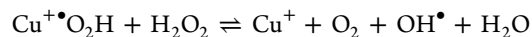
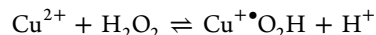
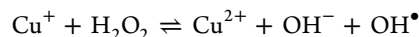
562 When Co(II) -based homogeneous catalysts are oxidized by
563 H_2O_2 , they can eventually form cobalt intermediate species
564 $[(\text{HOO})\text{L-Co(III)}]$ with catalytic activity. There are several
565 reports with spectroscopic evidence about intermediate
566 formation.^{38,39} In our heterogeneous system, both the
567 $[(\text{HOO})\text{L-Co(III)}]$ intermediate and the radicals could
568 eventually react with organic substrates.

569 In the same way, the $\text{Cu(II)-poly(EGDE-DA)}/\text{H}_2\text{O}_2$
570 heterogeneous system produced gas bubbles and free radicals
571 detected by spin trapping experiments with DMPO (Figure
572 3B). The pH did not vary significantly at the time that the
573 partial pressure of O_2 increased together with the concentration
574 of free radicals (Table S3 of the Supporting Information). The
575 simulation and fits of the experimental spectrum allowed for the
576 establishment of the presence of the DMPO/OH adduct from
577 OH^\bullet (Figure S11B of the Supporting Information).³⁶

On the basis of previous studies on H_2O_2 activation catalyzed
578 by copper complexes of EGDE-derived polymers,^{13,40,41} a
579 possible reaction could be
580



where the steps should be:



The Cu(I)-superoxide complex ($\text{Cu}^+\text{O}_2\text{H}$) should be in
582 equilibrium with the $\text{Cu}^{2+}(\text{O}_2\text{H})^-$ complex by the reversible
583 exchange of an electron. The occurrence of such transient
584 complexes has been proposed and discussed before.^{41,42}
585 Masarwa et al. determined that, in the mechanism of
586 “Fenton-like” reactions, the cation forms a transient complex
587 with H_2O_2 of the type $(\text{H}_2\text{O})_{m-1}\text{Cu}^+\text{O}_2\text{H}^-$, which can be
588 decomposed into $\text{Cu}(\text{H}_2\text{O})_m^{2+} + \text{OH}^\bullet$ or can react with an
589 organic substrate such as alcohol (ethanol, 2-propanol, or 2-
590 butanol).
591

3.9. Decolorization of Methyl Orange (MO). H_2O_2
592 activation by the poly(EGDE-DA) complexes with Co(II) and
593 Cu(II) was applied on the decolorization of MO solutions
594 (Scheme S1 of the Supporting Information).¹³
595

Without the nonsoluble polymer acting as a ligand, the
596 $\text{Co(II)}/\text{H}_2\text{O}_2$ and the $\text{Cu(II)}/\text{H}_2\text{O}_2$ systems only oxidized less
597 than 10% of the dye in 1 h.^{12,13}
598

In the presence of $\text{Co(II)-poly(EGDE-DA)}$ or Cu(II)-
599 poly(EGDE-DA) and H_2O_2 , the dye removal from the solution
600 was a consequence of two parallel processes: surface adsorption
601 on the catalyst and oxidative degradation, both of them
602 following pseudo-first-order kinetics.^{12,13} MO degradation is
603 expected to be slower than the adsorption process which only
604 involves mass transport and noncovalent bond formation.¹² In
605 agreement with this, we propose an empirical model where
606 each process is described by a pseudo-first order kinetic term,
607 assigning the term with the highest kinetic constant (k) to the
608 adsorption (Table 2):
609 12

$$[\text{MO}]_t = [\text{MO}]_{\text{ads}} \times e^{-k_{\text{ads}}t} + [\text{MO}]_{\text{deg}} \times e^{-k_{\text{deg}}t} + [\text{MO}]_{\infty} \quad (5)$$

where $[\text{MO}]_{\infty}$ represents the permanent free MO, $[\text{MO}]_{\text{ads}}$ is
611 the total amount of MO per liter of solution that would be
612 removed by adsorption, and $[\text{MO}]_{\text{deg}}$ is the total amount of
613 MO per liter of solution that would be removed by degradation.
614

Table 2. Estimated Parameters and Standard Deviation of the Pseudo-First Order Kinetic Model for the Decolorization of MO Solutions by Activation of H_2O_2 with $\text{Co(II)-poly(EGDE-DA)}$ or $\text{Cu(II)-poly(EGDE-DA)}$ ^a

| parameters | first catalytic cycle of $\text{Co(II)-poly(EGDE-DA)}$ [H_2O_2] ₀ : 63 mM | adsorption on $\text{Co(II)-poly(EGDE-DA)}$ in absence of H_2O_2 | first catalytic cycle of $\text{Cu(II)-poly(EGDE-DA)}$ [H_2O_2] ₀ : 63 mM | adsorption on $\text{Cu(II)-poly(EGDE-DA)}$ in absence of H_2O_2 |
|--|--|--|--|--|
| $[\text{MO}]_{\text{ads}}$ (μM) | 23.87 ± 0.30 | 28.23 ± 0.60 | 12.3 ± 1.4 | 19.46 ± 0.71 |
| k_{ads} (min^{-1}) | 0.2867 ± 0.0077 | 0.234 ± 0.012 | 2.9 ± 1.4 | 0.81 ± 0.06 |
| $[\text{MO}]_{\text{deg}}$ (μM) | 15.58 ± 0.25 | | 29.7 ± 1.3 | |
| k_{deg} (min^{-1}) | 0.0102 ± 0.0006 | | 0.175 ± 0.011 | |
| $[\text{MO}]_{\infty}$ (μM) | | 15.50 ± 0.44 | | 21.37 ± 0.18 |
| R^2 | 0.9972 | 0.9893 | 0.9957 | 0.9706 |

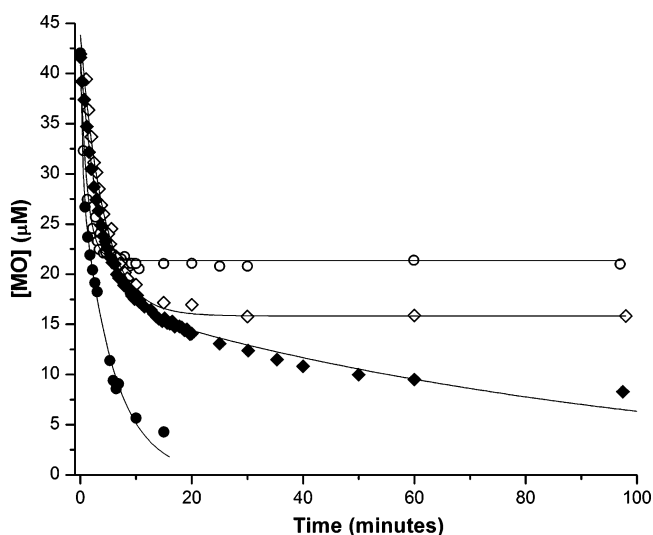
^aInitial MO concentration: 42 μM .

615 When Cu(II)-*poly*(EGDE-DA) was used, $[MO]_{\infty}$ repre-
 616 sented the free MO that was decomposed with a very low
 617 kinetic constant since complete removal was observed after 24
 618 h of reaction.

619 The first studies of interaction were performed in the
 620 absence of H_2O_2 , for a mass of complex (g) to volume of
 621 solution (L) ratio equal to 1.0 and an initial MO concentration
 622 of 42 μM . About 64.6% of the dye adsorbed on Co(II)-
 623 *poly*(EGDE-DA) and 47.7% on Cu(II)-*poly*(EGDE-DA)
 624 (Table 2).

625 The most probable binding sites of these negatively charged
 626 dye molecules are the $-R_2NH^+$ residues from DA and the
 627 adsorbed cations.

628 In the presence of 63 mM H_2O_2 , the amount of MO
 629 adsorbed was lower in both systems. The fraction of degraded
 630 MO by activated H_2O_2 was 40% with Co(II)-*poly*(EGDE-DA)
 631 and 71% with Cu(II)-*poly*(EGDE-DA). The parameter k_{deg}
 632 related to MO oxidation was 17.2 times higher for Cu(II)-
 633 *poly*(EGDE-DA) than for Co(II)-*poly*(EGDE-DA). Figure 4
 634 shows that 87% of MO was removed in 10 min with Cu(II)-
 635 *poly*(EGDE-DA); instead, it would take 110 min with Co(II)-
 636 *poly*(EGDE-DA).



637 **Figure 4.** MO concentration profile in the heterogeneous system,
 638 which consisted of 100 mL of 42 μM MO solution in contact with
 639 0.1000 g of the Co(II)-*poly*(EGDE-DA) and 63 mM H_2O_2 (\diamond), 0.1000
 640 g of the Co(II)-*poly*(EGDE-DA) (\blacklozenge), 0.1000 g of the Cu(II)-
 641 *poly*(EGDE-DA) and 63 mM H_2O_2 (\bullet), and 0.1000 g of the Cu(II)-
 642 *poly*(EGDE-DA) (\circ).

637 When the catalysts were recycled, the adsorption sites for
 638 MO remained occupied by the molecules bound on the first
 639 stage, at the time that $[MO]_{\infty}$ increased on the two successive
 640 cycles.

641 The UV-visible spectra of the MO solutions are presented
 642 in Figure S13 and Discussion of Figure S13 in the Supporting
 643 Information.

644 MO concentration was also monitored in the presence of
 645 *poly*(EGDE-DA) (Figure S14 of the Supporting Information).
 646 The amount of MO removed by adsorption on the positive
 647 surface of the polyelectrolyte was significantly higher than that
 648 adsorbed on the particles of the complexes. The addition of
 649 H_2O_2 produced the release of O_2 (Table S3 of the Supporting
 650 Information) and the decolorization of the solution by

adsorption (mostly), together with an alternative reaction 651
 which would involve the functional groups of the polyelec- 652
 trolyte ($-OH$, $-R_2N$, and $-O-$), and contributed only with 653
 8.41% of MO removal. 654

The normalized efficiency of Co(II)-*poly*(EGDE-DA) and 655
 Cu(II)-*poly*(EGDE-DA) was also compared. When we used 656
 equimolar amounts of catalytic sites in the medium of the 657
 reaction (0.644 mmol of sites per liter of MO solution), 40.9% 658
 of initial MO was decolorized by action of H_2O_2 with Co(II)- 659
poly(EGDE-DA) against 77.9% with Cu(II)-*poly*(EGDE-DA), 660
 and the k_{deg} was 1.66 times higher with the latter catalyst 661
 (Figure S15 of the Supporting Information). The control 662
 experiment in the absence of H_2O_2 showed 67.3% of MO 663
 adsorption on Co(II)-*poly*(EGDE-DA) against 39.5% on 664
 Cu(II)-*poly*(EGDE-DA), consistent with the larger mass of 665
 complex with Co(II) and the lower mass of complex with 666
 Cu(II) needed to obtain equimolar number of sites per volume 667
 of solution (Figure S15 of the Supporting Information). 668

At the light of these results, the catalyst with Cu(II) was 669
 clearly more efficient in terms of kinetics, and its lower ability 670
 to bind MO helped to minimize passivation of the active 671
 surface. 672

To improve the performance of Co(II)-*poly*(EGDE-DA) and 673
 evaluate the influence of additional solutes, the decolorization 674
 of MO was tested in two different reaction media: distilled 675
 water and 0.1 M Na_2SO_4 . The amount of decolorized MO by 676
 degradation increased 50% in the presence of inorganic salts, 677
 but k_{deg} was 3.39 times higher in distilled water. Even if the 678
 inorganic ions contributed to minimizing the adsorption, they 679
 exhibited some inhibitory effect on the chemical oxidation. 680
 Moreover, the chemical stability of Co(II)-*poly*(EGDE-DA) 681
 was affected in the presence of Na^+ and SO_4^{2-} , since a partial 682
 loss of complex was observed after the catalytic cycle. 683

The next experiments were conducted to evidence the 684
 mechanisms of MO degradation, the role of the solid matrix, 685
 and the potential participation of cobalt or copper intermediate 686
 species in the MO oxidative reaction (a possible metal-peroxo 687
 center). 688

We started with Co(II)-*poly*(EGDE-DA). First, the dye 689
 concentration in the H_2O_2 -activated supernatant was moni- 690
 tored as a function of time, exhibiting a pseudo-first-order 691
 exponential decay with k_{deg} equal to $(3.50 \pm 0.04) \times 10^{-3}$ 692
 min^{-1} (Figure S16 of the Supporting Information). This 693
 parameter was significantly lower (34.4%) than the kinetic 694
 constant estimated for the degradation process ($0.0102 \pm$ 695
 $0.0006 min^{-1}$) when the whole Co(II)-*poly*(EGDE-DA)/63 696
 mM H_2O_2 heterogeneous system was used (Table 2). 697

The behavior of Co(II)-*poly*(EGDE-DA) as catalyst differed 698
 from that of Co(II)-*poly*(EGDE-MAA-2MI), the complex 699
 between Co(II) and the nonsoluble polyampholyte mentioned 700
 in Introduction.¹² In a previous work, we demonstrated that the 701
 free radicals from the H_2O_2 supernatant activated by Co(II)- 702
poly(EGDE-MAA-2MI) were able to degrade MO with the 703
 same efficiency as the whole Co(II)-*poly*(EGDE-MAA-2MI)/ 704
 63 mM H_2O_2 heterogeneous system.¹² 705

Here, the chemical oxidation of MO in solution by the 706
 activated supernatant with one single catalytic cycle did not 707
 represent the whole process of dye degradation. It is possible 708
 that more catalytic cycles are needed to reach the efficiency of 709
 the Co(II)-*poly*(EGDE-DA)/63 mM H_2O_2 system. 710

The difference observed in the behavior of the catalysts is 711
 probably based on the nature of the ligand: *poly*(EGDE-MAA- 712
 2MI) is a polyampholyte combining positive and negative 713

714 charges on the same network, whereas *poly*(EGDE-DA) is a
 715 positive polyelectrolyte that exchanged H^+ for $Co(II)$ on the
 716 complex formation. So, species such as $O_2^{\bullet-}$ could be repelled
 717 out to the solution by the former and attracted by the latter on
 718 H_2O_2 activation.

719 Then, we looked for some evidence of $Co(II)$ intermediate
 720 species formed on the catalyst surface by action of H_2O_2 , acting
 721 as catalytic sites. The activated $Co(II)$ -*poly*(EGDE-DA)
 722 particles were put in contact with the MO solution, which
 723 exhibited a decrease in MO concentration following an
 724 exponential decay. In this experiment, the kinetics of the
 725 decolorization was mostly ruled by MO adsorption (Figure S16
 726 of the Supporting Information), giving no evidence of activity
 727 on the hypothetical first catalytic cycle.

728 Next, we explored the action of $Cu(II)$ -*poly*(EGDE-DA).
 729 The dye concentration in the activated H_2O_2 supernatant
 730 exhibited a pseudo-first order exponential decay with k_{deg} equal
 731 to $0.0415 \pm 0.0012 \text{ min}^{-1}$ (Figure S17 of the Supporting
 732 Information), 23.7% of the kinetic constant estimated for the
 733 degradation process ($0.175 \pm 0.011 \text{ min}^{-1}$) with the
 734 heterogeneous $Cu(II)$ -*poly*(EGDE-DA)/63 mM H_2O_2 system
 735 (Table 2).

736 On the other hand, the search for evidence of $Cu(II)$
 737 intermediate species on the surface of the particles led to a
 738 peculiar result: the amount of MO removed from the solution
 739 by the activated solid (37.1%) was lower than that removed by
 740 adsorption on the nonactivated catalyst (47.7%) (Figure S17 of
 741 the Supporting Information). This could be attributed to a
 742 decrease in the number of positive adsorption sites for the
 743 negatively charged MO as a result of the activation. Besides, this
 744 hypothetical $Cu(II)$ intermediate seems to be inactive in
 745 contact with MO.

746 In the same way, the sum of the effects of the activated
 747 supernatant and the activated solid on MO concentration
 748 (corresponding to a first catalytic cycle) did not explain the
 749 whole process of MO decolorization using $Cu(II)$ -*poly*(EGDE-
 750 DA).

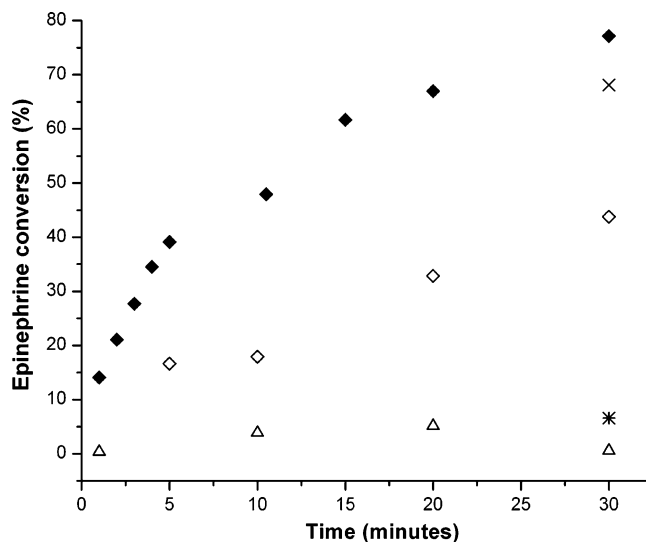
751 **3.10. Epinephrine Oxidation to Adrenochrome Using**
 752 **$Co(II)$ -*Poly*(EGDE-DA)/ H_2O_2 .** Epinephrine is a catecholamine,
 753 susceptible to peroxide attack. It can be partially oxidized by
 754 superoxide to the industrial pink product adrenochrome
 755 (catecholamine *o*-quinone; Scheme S1 in the Supporting
 756 Information), a precursor of hemostatic drugs such as
 757 carbazochrome.⁴³

758 Figure 5 presents the results of the epinephrine conversion in
 759 the presence of H_2O_2 and $Co(II)$ -*poly*(EGDE-DA). About 77%
 760 of conversion was reached in 30 min, with a pseudo-first-order
 761 kinetic constant of $0.145 \pm 0.019 \text{ min}^{-1}$.

762 In the absence of a catalyst, the oxidation of epinephrine by
 763 H_2O_2 was practically negligible.

764 A control experiment with epinephrine, H_2O_2 , and $Co(II)$ -
 765 *poly*(EGDE-DA), was made with previous bubbling of argon in
 766 the suspension of the complex to displace the dissolved O_2 and
 767 to saturate the atmosphere with the inert gas. Epinephrine
 768 conversion was found to be 11% lower than in the original
 769 reaction, meaning that H_2O_2 prevailed as oxidant and that the
 770 contribution of dissolved O_2 in epinephrine conversion was
 771 poor but evident.

772 Another control experiment performed with epinephrine and
 773 $Co(II)$ -*poly*(EGDE-DA) in the absence of H_2O_2 exhibited
 774 some extent of catecholamine oxidation, being less efficient
 775 than the oxidation by H_2O_2 . Then, the control experiment was
 776 repeated, this time with previous and continuous bubbling of



777 **Figure 5.** Epinephrine conversion: in the presence of $Co(II)$ -
 778 *poly*(EGDE-DA) (\blacklozenge), in the presence of $Co(II)$ -*poly*(EGDE-DA)
 779 with argon bubbling (*), in the presence of $Co(II)$ -*poly*(EGDE-DA)
 780 and 46 mM H_2O_2 with argon bubbling (x), and in the presence of 46
 781 mM H_2O_2 (Δ).

777 argon. Here, the amount of adrenochrome released was
 778 negligible, confirming that the oxidation of epinephrine could
 779 also be achieved with atmospheric O_2 when it was activated in
 780 some way by $Co(II)$ -*poly*(EGDE-DA). 780

781 4. CONCLUSIONS

782 The novel hydrogel *poly*(EGDE-DA) was synthesized in a one-
 783 step batch synthetic strategy using a diepoxy monomer
 784 (EGDE) and a bifunctional primary amine (DA). The material
 785 swelled in a wide range of pH below 10.5. Around 27% of the N
 786 atoms were tritrable basic sites, which acted as ligands together
 787 with the hydroxyl groups on $Co(II)$ and $Cu(II)$ coordination.
 788 The uptake capacity for $Cu(II)$ was 13.7 times higher than that
 789 for $Co(II)$, giving a more rigid material with better spectral
 790 resolution in FT-IR and *ss*-NMR analysis. 789

790 The catalytic activity of these coordination compounds on
 791 H_2O_2 activation was deeply studied by ESR. We propose a
 792 mechanism of reaction for each complex, which involves the
 793 simultaneous production of free radicals and O_2 . 793

794 The heterogeneous systems for H_2O_2 activation were tested
 795 on the oxidative degradation of the azo-dye MO. The complex
 796 with $Cu(II)$ was more efficient on dye decolorization. 796

797 The experiments conducted to evidence the activation of the
 798 solid matrix by H_2O_2 and the role of the free radicals in MO
 799 oxidative reaction showed that one single reaction cycle did not
 800 represent the whole process of dye degradation, being a key
 801 indicator of the catalytic activity of these nonsoluble organo-
 802 metallic compounds. 802

803 The utility of $O_2^{\bullet-}$ on partial oxidation reactions was
 804 demonstrated when the $Co(II)$ -*poly*(EGDE-DA)/ H_2O_2 hetero-
 805 geneous system was tested on the conversion of epinephrine to
 806 adrenochrome. In this case, we found that O_2 could also be
 807 activated by the complex. 807

808 Although the aim of this work was to prepare $Co(II)$ and
 809 $Cu(II)$ complexes of *poly*(EGDE-DA) that might be of interest
 810 in oxidation processes, there are many other possible uses of 810

811 this polyelectrolyte in recovery processes of low environmental
812 impact.

813 ■ ASSOCIATED CONTENT

814 ● Supporting Information

815 Titration curve; Cu(II) adsorption isotherm; TG-DTG/DSC
816 curves; FT-IR, EDS, and CW ESR spectra; H₂O₂ concentration
817 profile; MO concentration profiles and tables. This material is
818 available free of charge via the Internet at <http://pubs.acs.org>.

819 ■ AUTHOR INFORMATION

820 Corresponding Authors

821 *E-mail: lazarojm@ffy.uba.ar. Tel: +54-114-964-8200. Int.
822 8351.

823 *E-mail: vcldall@ffy.uba.ar. Tel: +54-114-964-8263. Fax: +54-
824 114-964-8263.

825 Notes

826 The authors declare no competing financial interest.

827 ■ ACKNOWLEDGMENTS

828 The authors thank the financial support from University of
829 Buenos Aires (UBACyT 10-12/237, 11-14/915, and 13-16/
830 021), CONICET (10-12/PIP 076), ANPCyT (BID Bicente-
831 nario/PICT 1957; PICT 2012 0151 and PICT 2012 0716).
832 L.V.L.L. thanks the CONICET for her doctoral fellowship. The
833 authors thank Dr. Victor Busto (Faculty of Pharmacy and
834 Biochemistry, University of Buenos Aires) for the measure-
835 ments of partial pressure of O₂.

836 ■ REFERENCES

- 837 (1) Anderson, E. B.; Long, T. E. Imidazole- and imidazolium-
838 containing polymers for biology and material science applications.
839 *Polymer* **2010**, *51*, 2447–2454.
- 840 (2) Campbell, V. E.; Chiarelli, P. A.; Kaur, S.; Malkiat, S.
841 Coadsorption of a polyanion and an azobenzene dye in self-assembled
842 and spin-assembled polyelectrolyte multilayers. *Chem. Mater.* **2005**, *17*,
843 186–190.
- 844 (3) Kabanov, A. V.; Vinogradov, S. V. Nanogels as pharmaceutical
845 carriers: Finite networks of infinite capabilities. *Angew. Chem., Int. Ed.*
846 **2009**, *48*, 5418–5429.
- 847 (4) Liu, Y.; Ogawa, K.; Schanze, K. S. Conjugated polyelectrolytes as
848 fluorescent sensors. *J. Photochem. Photobiol., C* **2009**, *10*, 173–190.
- 849 (5) Leal Denis, M. F.; Carballo, R. R.; Spiaggi, A. J.; Dabas, P. C.;
850 Campo Dall'Orto, V.; Lázaro Martínez, J. M.; Buldain, G. Y. Synthesis
851 and sorption properties of a polyampholyte. *React. Funct. Polym.* **2008**,
852 *68*, 169–181.
- 853 (6) Lázaro Martínez, J. M.; Leal Denis, M. F.; Campo Dall'Orto, V.;
854 Buldain, G. Y. Synthesis, FT IR, solid state NMR and SEM studies of
855 novel polyampholytes or polyelectrolytes obtained from EGDE, MAA
856 and imidazoles. *Eur. Polym. J.* **2008**, *44*, 392–407.
- 857 (7) Lázaro Martínez, J. M.; Chattah, A. K.; Monti, G. A.; Leal Denis,
858 M. F.; Buldain, G. Y.; Campo Dall'Orto, V. New copper(II)
859 complexes of polyampholyte and polyelectrolyte polymers: Solid-state
860 NMR, FT-IR, XRPD and thermal analyses. *Polymer* **2008**, *49*, 5482–
861 5489.
- 862 (8) Lázaro Martínez, J. M.; Chattah, A. K.; Torres Sánchez, R. M.;
863 Buldain, G. Y.; Campo Dall'Orto, V. Synthesis and characterization of
864 novel polyampholyte and polyelectrolyte polymers containing
865 imidazole, triazole or pyrazole. *Polymer* **2012**, *53*, 1288–1297.
- 866 (9) Lázaro Martínez, J. M.; Monti, G. A.; Chattah, A. K. Insights into
867 the coordination sphere of copper ion in polymers containing
868 carboxylic acid and azole groups. *Polymer* **2013**, *54*, 5214–5221.
- 869 (10) Annenkov, V. V.; Danilovtseva, E. N.; Saraev, V. V.; Mikhaleva,
870 A. I. Complexation of copper(II) ions with imidazole–carboxylic

- polymeric systems. *J. Polym. Sci., Part A: Polym. Chem.* **2003**, *41*, 871
2256–2263. 872
- (11) Pithadia, A. S.; Lim, M. H. Metal-associated amyloid- β species in
873 Alzheimer's disease. *Curr. Opin. Chem. Biol.* **2012**, *16*, 67–73. 874
- (12) Lombardo Lupano, L. V.; Lázaro Martínez, J. M.; Piehl, L. L.;
875 Rubín de Celis, E.; Campo Dall'Orto, V. Activation of H₂O₂ and
876 superoxide production using a novel cobalt complex based on a
877 polyampholyte. *Appl. Catal., A* **2013**, *467*, 342–354. 878
- (13) Lázaro Martínez, J. M.; Leal Denis, M. F.; Piehl, L. L.; Rubín de
879 Celis, E.; Buldain, G. Y.; Campo Dall'Orto, V. Studies on the
880 activation of hydrogen peroxide for color removal in the presence of a
881 new Cu(II)-polyampholyte heterogeneous catalyst. *Appl. Catal., B*
882 **2008**, *82*, 273–283. 883
- (14) Jones, C. W. *Applications of Hydrogen Peroxide and Derivatives*;
884 RSC: London, 1999. 885
- (15) Oller, I.; Malato, S.; Sánchez-Pérez, J. A. Combination of
886 advanced oxidation processes and biological treatments for wastewater
887 decontamination: A review. *Sci. Total Environ.* **2011**, *409*, 4141–4166. 888
- (16) Carabineiro, S. A. C.; Martins, L. M. D. R. S.; Avalos-Borja, M.;
889 Buijnsters, J. G.; Pombeiro, A. J. L.; Figueiredo, J. L. Gold
890 nanoparticles supported on carbon materials for cyclohexane oxidation
891 with hydrogen peroxide. *Appl. Catal., A* **2013**, *467*, 279–290. 892
- (17) Fung, B. M.; Khitrin, A. K.; Ermolaev, K. An improved
893 broadband decoupling sequence for liquid crystals and solids. *J. Magn.*
894 *Reson.* **2000**, *142*, 97–101. 895
- (18) Lamas, M. C.; Torres Sánchez, R. M. Isoelectric point of soils
896 determined by the diffusion potential method. *Geoderma* **1998**, *85*,
897 371–381. 898
- (19) El-Brashy, A. M.; El-Sayed Metwally, M.; El-Sepai, F. A.
899 Spectrophotometric determination of some fluoroquinolone anti-
900 bacterials by ion-pair complex formation with cobalt (II) tetrathio-
901 cyanate. *J. Chin. Chem. Soc.* **2005**, *52*, 77–84. 902
- (20) Hadi, M.; Samarghandi, M. R.; McKay, G. Equilibrium two-
903 parameter isotherms of acid dyes sorption by activated carbons: Study
904 of residual errors. *Chem. Eng. J. (Amsterdam, Neth.)* **2010**, *160*, 408–
905 416. 906
- (21) Copello, G. J.; Díaz, L. E.; Campo Dall'Orto, V. Adsorption of
907 Cd(II) and Pb(II) onto a one step-synthesized polyampholyte. Kinetics
908 and equilibrium studies. *J. Hazard. Mater.* **2012**, *217*, 374–
909 381. 910
- (22) Ettinger, M. B.; Ruchhoft, C. C.; Lishka, R. J. Sensitive 4-
911 aminoantipyrine method for phenolic compounds. *Anal. Chem.* **1951**,
912 *23*, 1783–1788. 913
- (23) Kokufuta, E. Polyelectrolyte gel transitions: experimental
914 aspects of charge inhomogeneity in the swelling and segmental
915 attractions in the shrinking. *Langmuir* **2005**, *21*, 10004–10015. 916
- (24) Guo, X.; Ballauff, M. Spherical polyelectrolyte brushes:
917 Comparison between annealed and quenched brushes. *Phys. Rev. E*
918 **2001**, *64*, 051406/1–051406/9. 919
- (25) Patrickios, C. S.; Simmons, M. R. Synthesis and aqueous
920 solution characterization of catalytically active homopolymers, block
921 copolymers and networks containing imidazole. *Colloids Surf., A* **2000**,
922 *167*, 61–72. 923
- (26) Aharoni, C.; Sparks, D. L. Kinetics of soil chemical reactions: A
924 theoretical treatment. In: Sparks, D. L.; Suarez, D. L. (Eds.) *Rates of*
925 *Soil Chemical Processes*; Soil Science Society of America: Madison, WI,
926 1991, pp 1–18. 927
- (27) Hsieh, C.-T.; Teng, H. Langmuir and Dubinin–Radushkevich
928 analyses on equilibrium adsorption of activated carbon fabrics in
929 aqueous solutions. *J. Chem. Technol. Biotechnol.* **2000**, *75*, 1066–1072. 930
- (28) Hobson, J. P. Physical adsorption isotherms extending from
931 ultrahigh vacuum to vapor pressure. *J. Phys. Chem.* **1969**, *73*, 2720–
932 2727. 933
- (29) Gubbük, I. H.; Güp, R.; Ersöz, M. Synthesis, characterization,
934 and sorption properties of silica gel-immobilized Schiff base derivative.
935 *J. Colloid Interface Sci.* **2008**, *320*, 376–382. 936
- (30) Wu, K. H.; Chang, T. C.; Wang, Y. T.; Hong, Y. S.; Wu, T. S.
937 Interactions and mobility of copper(II)–imidazole-containing copoly-
938 mers. *Eur. Polym. J.* **2003**, *39*, 239–245. 939

- 940 (31) Chiu, Y. S.; Wu, K. H.; Chang, T. C. Miscibility and dynamics of
941 the poly(vinylimidazole-co-methyl methacrylate)–silica hybrids stud-
942 ied by solid-state NMR. *Eur. Polym. J.* **2003**, *39*, 2253–2259.
- 943 (32) Belfiore, L. A.; McCurdie, M. P.; Das, P. K. Macromolecule–
944 metal complexes: ligand field stabilization and thermophysical
945 property modification. *Polymer* **2001**, *42*, 9995–10006.
- 946 (33) McCurdie, M. P.; Belfiore, L. A. Spectroscopic analysis of
947 transition-metal coordination complexes based on poly(4-vinyl-
948 pyridine) and dichlorotricarbonylruthenium(II). *Polymer* **1999**, *40*,
949 2889–2902.
- 950 (34) Santana, A. L.; Noda, L. K.; Pires, A. T. N.; Bertolino, J. R. Poly
951 (4-vinylpyridine)/cupric salt complexes: Spectroscopic and thermal
952 properties. *Polym. Test.* **2004**, *23*, 839–845.
- 953 (35) Rouquerol, J.; Avnir, D.; Fairbridge, C. W.; Everett, D. H.;
954 Haynes, J. H.; Pernicone, N.; Ramsay, J. D. F.; Sing, K. S. W.; Unger,
955 K. K. Recommendations for the characterization of porous solids. *Pure*
956 *Appl. Chem.* **1994**, *66*, 1739–1758.
- 957 (36) Buettner, G. R. Spin Trapping: ESR parameters of spin adducts
958 1474 1528V. *Free Radical Biol. Med.* **1987**, *3*, 259–303.
- 959 (37) Liang, S.-X.; Zhao, L.-X.; Zhang, B.-T.; Lin, J.-M. Experimental
960 studies on the chemiluminescence reaction mechanism of carbonate/
961 bicarbonate and hydrogen peroxide in the presence of cobalt(II). *J.*
962 *Phys. Chem. A* **2008**, *112*, 618–623.
- 963 (38) Shen, C.; Song, S.; Zang, L.; Kang, X.; Wen, Y.; Liu, W.; Fu, L.
964 Efficient removal of dyes in water using chitosan microsphere
965 supported cobalt (II) tetrasulfophthalocyanine with H₂O₂. *J. Hazard.*
966 *Mater.* **2010**, *177*, 560–566.
- 967 (39) Agboola, B.; Ozoemena, K. I.; Nyokong, T. Hydrogen peroxide
968 oxidation of 2-chlorophenol and 2,4,5-trichlorophenol catalyzed by
969 monomeric and aggregated cobalt tetrasulfophthalocyanine. *J. Mol.*
970 *Catal. A: Chem.* **2005**, *227*, 209–216.
- 971 (40) Lázaro Martínez, J. M.; Rodríguez-Castellón, E.; Torres
972 Sánchez, R. M.; Denaday, L. R.; Buldain, G. Y.; Campo Dall’Orto,
973 V. XPS studies on the Cu(I,II)–polyampholyte heterogeneous
974 catalysts: An insight into its structure and mechanism. *J. Mol. Catal.*
975 *A: Chem.* **2011**, *339*, 43–51.
- 976 (41) Pecci, L.; Montefoschi, G.; Cavallini, D. Some new details of the
977 copper-hydrogen peroxide interaction. *Biochem. Biophys. Res. Commun.*
978 **1997**, *235*, 264–267.
- 979 (42) Masarwa, M.; Cohen, H.; Meyerstein, D.; Hickman, D. L.;
980 Bakac, A.; Espenson, J. H. Reactions of low-valent transition-metal
981 complexes with hydrogen peroxide. Are they “Fenton-like” or not? 1.
982 The case of Cu⁺aq and Cr²⁺aq. *J. Am. Chem. Soc.* **1988**, *110*, 4293–
983 4297.
- 984 (43) Alhasan, R.; Njus, D. The epinephrine assay for superoxide:
985 Why dopamine does not work. *Anal. Biochem.* **2008**, *381*, 142–147.